forces, it is desirable to locate their position accurately. The breaks occurring at palladium, tungsten and lead have been checked by using the Wesleyan University mass spectrograph to search for certain unobserved isotopes of these elements, namely, Pd^{100}, W^{178} and Pb^{202}.

The isotopic constitution of palladium was determined by Dempster[2] in 1935 and an electrical measurement of the isotopic abundances was made by Sampson and Bleakney[3] in the following year. The faintest isotope, Pd^{102}, was found to have an abundance of 0.8 percent. In the present search for Pd^{100}, palladium ions were obtained from a high frequency spark between palladium electrodes. With an exposure of three hours no isotopes of palladium lighter than Pd^{102} were observed on the mass spectrum. On the other hand, Pd^{102} was clearly visible with an exposure of ten seconds. It is concluded that the hypothetical Pd^{100} exists to less than 0.0007 percent. The same limit of abundance can be assigned to Pd^{98}, Pd^{99} and Pd^{101}.

Tungsten is known to consist of five isotopes with mass numbers 180, 182, 183, 184 and 186. Of these, W^{180}, first observed by Dempster[4] in 1937, is much the rarest, constituting, according to Inghram,[5] 0.12 percent of normal tungsten. Although the hypothetical W^{178} has been shown by Inghram to exist to less than 0.002 percent, because of its unique position on the stability curve, a further search for it was made. Tungsten ions were obtained from a high frequency spark between two tungsten electrodes. An exposure of one minute showed the faint W^{180} while an exposure of two hours failed to reveal any isotopes lighter than this. It is concluded that the limit of abundance of W^{178} is 0.001 percent. Also, Inghram's limits of abundance can be lowered to 0.001 percent for both W^{179} and W^{181}.

Lead has four isotopes of which the lightest, Pb^{204}, is the least abundant, constituting, according to Nier,[6] 1.5 percent of normal lead. Using a spark between pure lead electrodes as a source of lead ions, a two-hour exposure failed to reveal any isotopes lighter than Pb^{204}. Pb^{204} itself was clearly visible with an exposure of one second. The limit of abundance of the hypothetical Pb^{202} is reckoned to be 0.0004 percent. The same limit holds for Pb^{203}, Pb^{201} and Pb^{200}.

On the basis of this search it seems reasonable to conclude that stable Pd^{100}, W^{178} and Pb^{202} do not exist. Such a conclusion permits the accurate location of three breaks in the above-mentioned stability curve.

The authors wish to thank Mr. Clifford Geiselbreth for his help in the making of electrodes.

* This letter is based on work done at Wesleyan University under Contract AT(30-1)-451 with the Atomic Energy Commission.

[1] H. E. Duckworth, Phys. Rev. **75**, 1438 (1949).
[2] A. J. Dempster, Nature **136**, 65 (1935).
[3] Milo B. Sampson and Walter Bleakney, Phys. Rev. **50**, 732 (1936).
[4] A. J. Dempster, Phys. Rev. **52**, 1074 (1937).
[5] M. G. Inghram, Phys. Rev. **70**, 653 (1946).
[6] A. O. Nier, J. Am. Chem. Soc. **60**, 1571 (1938).

Concentrating Holes and Electrons by Magnetic Fields

H. SUHL AND W. SHOCKLEY
Bell Telephone Laboratories, Murray Hill, New Jersey
March 24, 1949

IN the Hall effect for electrons alone or holes alone the carriers flow parallel to the specimen and the electric field has a transverse component. When both carriers are present, the net transverse current is zero due to compensating flows of holes and electrons to the same side. For low electric fields, recombination and generation keep the concentrations at their equilibrium values. Holes injected by transistor action at e in Fig. 1 were largely concentrated on one side of the germanium filament by virtue of the high electric fields ($\sim$20 v/cm) and small dimensions employed.

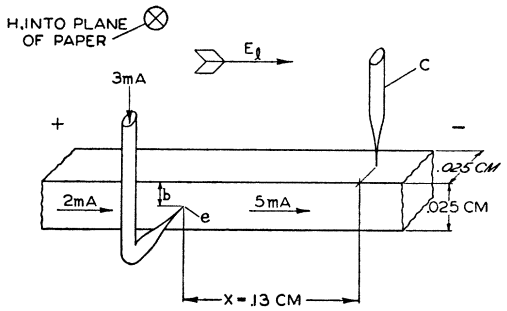

FIG. 1. Experimental arrangement of specimen, currents, and electric and magnetic fields.

The hole concentration at a distance x from the emitter was measured with the aid of a collector point c operated in the reverse direction so as to draw 10 μa. Figure 2 shows the conductance of this point *versus* H for the current conditions shown in Fig. 1. The conductance in excess of the value for $H=-20{,}000$ gauss is considered as proportional to hole concentration and is denoted by g on the left scale. Plus magnetic fields tend to concentrate holes on the collector side and the admittance rises; however, for $H>10{,}000$, the holes are concentrated near the surface and recombine with electrons on the surface so that the hole current decays before reaching c, and g decreases. For minus H, the holes are deflected away from c and g decreases monotonically.

The equations for p, the concentration of holes, are readily derived for: (1) hole concentration much less than electron concentration, (2) equal mobilities and concentrations for holes and electrons; in this case the space charges cancel, producing no transverse field. For (1) the transverse forces on the holes are approximated by a transverse electric field $E_2=E_l\sin(\theta_p+\theta_n)\cong E_l(\theta_p+\theta_n)$, where E_l is the longitudinal electric field $\theta_{p,n}=10^{-8}(R\sigma)_{p,n}H$ and $(R\sigma)_{n,p}=$mobility for electrons and holes ($\cong$1700 cm^2/v sec. for holes), and H is the magnetic field. (For (2), $E_2\cong E_l\theta_p$.) $\varphi=eE_2b/2kT\equiv KE_lH$, where $2b$ is the width of the filament, is a measure of the transverse concentration.

Recombination of holes with electrons on the surface of the filament takes place according to the law (component of hole flux normal to surface) $=s$ times (concentration of holes at the surface). For $H=0$ the concentration across the filament varies as $\cos\beta y$, where y is measured from the center and $\beta b\tan\beta b=sb/D\equiv\psi$, where $D=$diffusion constant.

For the following limiting cases, the values of p are:

for $\varphi\ll1$	$p=1+\varphi+(\varphi/\psi)\sin^2\beta b$,
large $+H$, $\varphi>1$	$p_+=[(4\varphi/\psi)-2]\exp[-A\psi(2\varphi-1)]$,
large $-H$	$p_-=p_+[1-(\psi/\varphi)]\exp(2\psi-4\varphi)$,

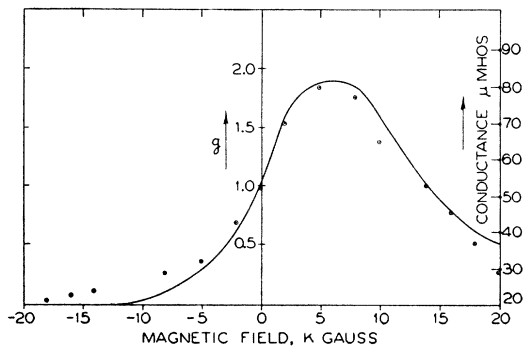

FIG. 2. Conductance of collector point, taken as measure of hole density, *versus* magnetic field.

where $A=(kTx/eE_1b^2)$. The curve of Fig. 2 corresponds to $A=2$, $\psi=0.43$, $K=10^{-5}$ cm/v gauss, assuming p proportional to g.

The value of s is about 1500 cm/sec., which implies that since thermal velocity is 10^7 cm/sec., a hole makes about 1500 collisions with the surface before being captured.

For H more negative than -8000 gauss, the curve does not fit the data. The difference is attributed to holes generated on the same surface as the collector. If these gave a contribution g_0 for $H=0$, they should contribute $g_0\psi/2\varphi$ for large negative H and thus give the hyperbolic tail observed.

It is evident that this technique, in addition to demonstrating concentration by magnetic fields and measuring surface recombination, can be used in the intrinsic range to measure ratios of holes to electrons and volume recombination constants.

The reduction of hole lifetime by strong magnetic fields accounts for large apparent magnetoresistive effects under conditions of hole injection.

We are indebted to G. L. Pearson whose development of and experiments with the filament technique suggested this experiment, and to J. R. Haynes and other colleagues at the Laboratories for many helpful suggestions.

Angular Correlations in Successive Nuclear α-γ-Emission and the Excited State of Li^7 *

BERNARD T. FELD

Physics Department and Laboratory for Nuclear Science and Engineering, Massachusetts Institute of Technology, Cambridge, Massachusetts

March 31, 1949

THE ~480-kev excited state of Li^7 has been observed in a variety of nuclear reactions.[1] Most of the data are consistent with the Li^7 level scheme (1) of Fig. 1. However, as pointed out by Inglis,[2] the α-particle branching, in the reaction $B^{10}(n,\alpha)Li^{7*}$, Li^7, is inconsistent with scheme (1); Inglis has suggested scheme (2), to explain this reaction.

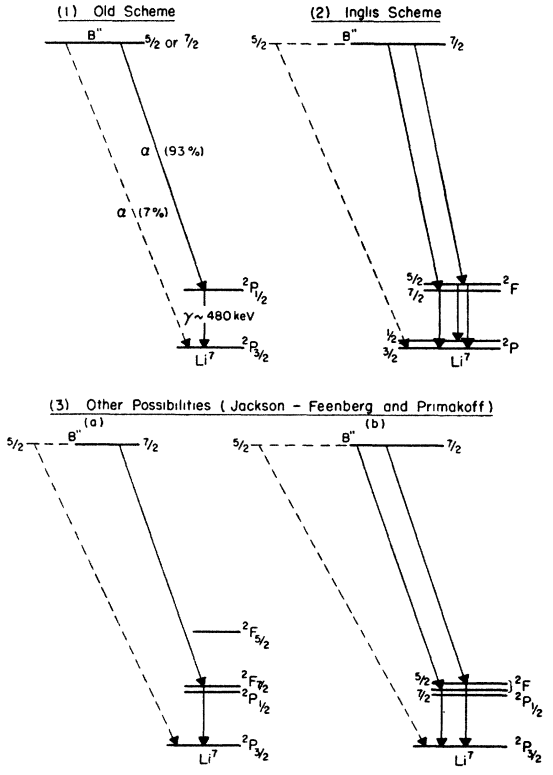

FIG. 1. Proposed level schemes for the $B^{10}(n,\alpha)Li^7$ reaction.

TABLE I. Theoretical angular correlations in successive α-γ-emission.

Initial (B^{11}) spin	α-particle angular momentum (L)	Intermediate (Li^{7*}) spin	γ-ray type	Final (Li^7) spin	$W(\theta)$
5/2 or 7/2	any	1/2	any	3/2	1
7/2	1	7/2	El. Quad.	3/2	$1-0.508\cos^2\theta$
7/2	1	5/2	El. Quad.	3/2	$1+0.079\cos^2\theta$
7/2	1	5/2	El. Quad.	1/2	$1+0.231\cos^2\theta$
7/2	1	5/2	El. Quad.	3/2 or 1/2	$1+0.197\cos^2\theta$
7/2	1	5/2	Mag. Dip.	3/2	$1-0.143\cos^2\theta$

Scheme (2) is, however, incapable of explaining the observed (~10 percent) branching in the Be^7 (K capure) Li^{7*}, Li^7 disintegration.[3] Scheme (3a) of Fig. 1, suggested by J. D. Jackson and by E. Feenberg and H. Primakoff,[4] has the advantage that it is consistent with the observations in both of the aforementioned reactions; scheme (3b), while less likely, is also consistent. However, these schemes depend on a fortuitous near-degeneracy of a number of levels.

It is the purpose of this note to suggest a method for distinguishing between the various suggested level schemes. Since the lifetime of the Li^{7*} state produced by the (thermal neutron) $B^{10}(n,\alpha)$ reaction is short ($<2\times10^{-13}$ sec.),[5] compared to the period associated with the Li^7 hyperfine structure splitting (~10^{-9} sec.),[6] the angular correlation between the directions of emission of the short-range α-particle (by B^{11}) and the ~480-kev γ-ray (by Li^{7*}), should depend on the spins of the states involved and on the angular momentum properties of the α-particle and γ-ray. Table I summarizes the expected angular correlations for the various possibilities shown in Fig. 1. $W(\theta)$ represents the relative number (per unit solid angle) of γ-rays emitted at an angle θ with respect to the preceding α-particle. The angular correlations were computed by the method of Hamilton,[7] suitably modified to take into account that the first particle emitted is an α-particle.

Of the schemes shown in Fig. 1, only (1) and (3a) lead to unambiguous answers. Scheme (1)—$^2P_{\frac{1}{2}}$ excited state—leads to $W(\theta)=1$, irrespective of the properties of the other two states or of the nature of the emitted particles, because of the symmetry associated with the spin $\frac{1}{2}$. Scheme (3a) results in a large angular correlation, with $W(0)/W(\pi/2)=0.492$, which should be easily observable.

The correlations for schemes (2) and (3b) depend on the relative branching of the α-particles to the two states of the F doublet. The branching of the γ-rays from the $^2F_{5/2}$ state to the P doublet (scheme 2) is uniquely determined by the properties of these states and the "sum rule";[8] the effect of this branching is shown in the last row of Table I. However, because the nature of the B^{11} state is not uniquely determined, the α-particle branching cannot be decided on purely theoretical grounds. Assuming relative probabilities of a and $(1-a)$, respectively, for the $7/2\rightarrow5/2$ and $7/2\rightarrow7/2$ transitions, we obtain

$$W(\theta)=1+(0.705a-0.508)\cos^2\theta, \text{ for scheme (2),}$$

and

$$W(\theta)=1+(0.587a-0.508)\cos^2\theta, \text{ for scheme (3b).}$$

Unfortunately, both of these possibilities lead to small angular correlations over certain ranges of values of a. If a difference of less than 10 percent between the correlations at angles 0 and $\pi/2$ were unobservable, the ranges $a=0.58-0.86$ for scheme (2) and $a=0.7-1.0$ for scheme (3b) would lead to apparent spherical symmetry. However, over most of the range of possible values of a, the angular correlation is easily observable.

Experiments are now under way at this laboratory to measure the α-γ-angular correlation in the $B^{10}(n,\alpha)Li^{7*}$ reaction. The α-particles are detected in a proportional